

See discussions, stats, and author profiles for this publication at: <https://www.researchgate.net/publication/328673143>

Video Processing and Analysis for Endoscopy-Based Internal Pipeline Inspection

Article in *Advances in Intelligent Systems and Computing* · January 2019

DOI: 10.1007/978-3-030-03658-4_6

CITATIONS

0

READS

361

3 authors:



Nafaa Nacereddine

Research Center In Industrial Technologies

56 PUBLICATIONS 392 CITATIONS

[SEE PROFILE](#)



Aissa Boulmerka

Centre universitaire de Mila

12 PUBLICATIONS 51 CITATIONS

[SEE PROFILE](#)



Nadia Mhamda

Research Center In Industrial Technologies

3 PUBLICATIONS 0 CITATIONS

[SEE PROFILE](#)

Some of the authors of this publication are also working on these related projects:



Journal of Innovative Applied Mathematics and Computational Sciences (JIAMCS) [View project](#)



Image segmentation [View project](#)



Video Processing and Analysis for Endoscopy-Based Internal Pipeline Inspection

Nafaa Nacereddine¹(✉), Aissa Boulmerka², and Nadia Mhamda¹

¹ Research Center in Industrial Technologies CRTI, 16014 Algiers, Algeria
{n.nacereddine,n.mhamda}@crti.dz

² DMI, Centre Universitaire de Mila, 43000 Mila, Algeria
a.boulmerka@centre-univ-mila.dz

Abstract. Because of the increasing requirements in regards to the pipeline transport regulations, the operators take care to the rigorous application of checking routines that ensure nonoccurrence of leaks and failures. In situ pipe inspection systems such as endoscopy, remains a reliable mean to diagnose possible abnormalities in the interior of a pipe such as corrosion. Through digital video processing, the acquired videos and images are analyzed and interpreted to detect the damaged and the risky pipeline areas. Thus, the objective of this work is to bring a powerful analysis tool for a rigorous pipeline inspection through the implementation of specific algorithms dedicated to this application for a precise delimitation of the defective zones and a reliable interpretation of the defect implicated, in spite of the drastic conditions inherent to the evolution of the endoscope inside the pipeline and the quality of the acquired images and videos.

1 Introduction

The pipelines are most likely to be attacked by corrosion, cracking or manufacturing defect, resulting sometimes in catastrophic damage (human damage, environmental pollution, additional repair costs, extended pumping shutdown, etc.). Consequently, the operators ensure rigorous monitoring schedule to prevent occurrence of any breakdown due to fluid leaks. Nowadays, such a situation poses increasingly severe requirements in terms of rules and standards governing the fluid pipe transport. For the purpose mentioned above, in situ pipe inspection systems such as endoscopy, remains a reliable mean to diagnose possible abnormalities in the interior of a pipe such as corrosion. The latter is defined as the breaking down or destruction of material, especially a metal through oxidation or chemical reactions [1]. The corrosion attacks remain the principal cause of fluid leaks and pipeline breaks.

In this work, the endoscope consists in a motorized engine equipped with a digital camera. The recovered videos and images inside the inspected pipelines

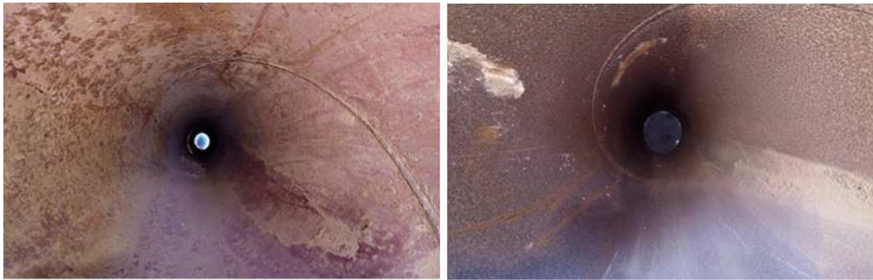


Fig. 1. Examples of corrosion in water transport pipelines

are analyzed and interpreted using digital video processing to detect the damaged and risky areas such as cracks, corrosion, lack of thickness, etc. To this end, the main stages of this work consist in: (1) designing and conceiving an automated motorized engine with embedded camera where the control is insured by Field Programmable Gate Arrays (FPGA) technology, and (2) implementing image/video processing and analysis software for an accurate detection and reliable identification and interpretation of the defective or risky areas such corrosion, found inside the pipeline, as illustrated in Fig. 1.

2 Motorized Vehicle Setup

In case of large pipeline, a vehicle controlled remotely, equipped with a camera, remains a practical solution, timely and interesting in order to perform internal inspection. The automated engine permits to provide real-time feedbacks to the user in terms of internal pipe video sequences to be analysed, distance travelled inside the pipeline, time spent, etc. In this work, to control the engine and the camera, we opt for the FPGA technology since, unlike hard-wired printed circuit board designs, these circuits provide several advantages such as hardware parallelism, flexibility, rapid prototyping capabilities, short time to market, reliability, long-term maintenance, etc. [2]. The realized pipeline endoscope is called “Pipe Explorer” where, the stepper motors driving the wheels are controlled by Zedboard (Xilinx Zynq-7000) FPGA card while the embedded CCD camera acquiring the videos is controlled by MicroZed FPGA card. “Pipe Explorer” is composed of:

- 4 wheels
- 4 stepper motors (1.8° /step) rotating on 360°
- 4 drivers microstep (JK 1545), DC power input type: 24V 50VDC. Output current: 1.3A–4.5A
- 1 EPL camera USB with 2 megapixel of resolution
- Lighting sources through 12 LEDs (12V) Samsung
- 3 Lead batteries rechargeable of capacity 12V/9Ah each, for the motors supply

- 2 Lithium batteries of capacity 12V/11Ah each, to supply Zedboard and MicroZed cards
- 1 Lithium battery 12v/11 A to supply the LEDs

For the endoscope thus realized, as shown in Fig. 2, the following characteristics are noted:

- Dimensions: 30cm × 33 cm × 54 cm
- Weight: 25 kg
- Autonomy: 6 h for a run of 2 km.



Fig. 2. The endoscope “Pipe-Explorer”

3 Video Analysis Software

In the context of pipeline inspection by endoscopy, we have developed software including video processing and analysis techniques in order to interpret the acquired videos. It is a question here of videos acquired inside the water transportation pipelines which, after a certain time of service, are prone to different types of attacks and degradations, particularly, corrosion. It is thus important to determine its localization, its extent and its degree of severity in order to take appropriate corrective action. Since the corroded part changes its appearance with respect to the rest of the pipeline, the frames or images forming the video sequence must be exploited using image segmentation techniques in order to extract the object representing corrosion, i.e. the defective area, from the background representing the undamaged region of the pipe. In fact, the segmentation constitutes one of the most significant problems in the image analysis system, because the result obtained at the end of this stage strongly governs the final quality of interpretation [3]. Color is a distinctive parameter that can be used to extract the corroded area from the rest of the internal pipeline view. Since these color images can be converted into grayscale images, thresholding techniques become a strong candidate for efficient segmentation. Thresholding is the

process of partitioning pixels in the images into object and background classes based upon the relationship between the gray level value of a pixel and a parameter called the threshold. Because of their efficiency in performance and their simplicity in theory, thresholding techniques have been studied extensively and a large number of thresholding methods have been published [4, 5]. Generally, for the images obtained from the video sequence acquired inside the pipeline, the overlapping between the corroded region and the background representing the healthy areas is large. This is due to the luminance variability of the corrosion and the background areas, in addition of the presence of artifacts. In such case, by a global thresholding, we do not obtain the desired results. That is why a local adaptive thresholding technique can be employed to overcome the above-mentioned problem.

In locally adaptive thresholding, the threshold value $T(x, y)$ is computed on the neighborhood of the current pixel (x, y) , i.e.

$$b(x, y) = \begin{cases} 0 & \text{if } f(x, y) < T(x, y) \\ 1 & \text{otherwise} \end{cases} \quad (1)$$

where, f is the input grayscale image and b is the output binary image.

In order to compute the threshold $T(x, y)$, the local mean $\mu(x, y)$ and the standard deviation $\sigma(x, y)$ have to be computed in a $W \times W$ window centered around each pixel (x, y) . In this paper, the method of Sauvola [6], which is an improved version of the method of Niblack [7], and the method of Feng [8], which is an improved version of the method of Wolf [9], are applied to detect in-situ pipeline corrosion and are compared in terms of detection efficiency.

3.1 Sauvola Thresholding Method

The main idea of Niblack's thresholding method [6] is to vary the threshold value, for each pixel (x, y) , over the input image of size $(M \times N)$, based on the local mean $\mu(x, y)$ and the local standard deviation $\sigma(x, y)$ in a $W \times W$ window centered around the pixel (x, y) . The threshold value at pixel (x, y) is computed by $T(x, y) = \mu(x, y) + k \times \sigma(x, y)$ where, k is a parameter which depends on image content. The parameters W and k are chosen empirically. This method tends to produce a big amount of noise, particularly, when the image background contains light textures, which are considered as object with small contrast. To overcome the above mentioned problems, Sauvola et al. [6] proposed an improved formula to compute the threshold

$$T(x, y) = \mu(x, y) \left(1 - k \left(1 - \frac{\sigma(x, y)}{R} \right) \right) \quad (2)$$

where R is the dynamic range of standard deviation and k a parameter which takes positive values in the range [0.2 0.5]. In this method, the parameter k controls the value of the threshold in the local window such that the higher the value of k , the lower the threshold from the local mean $\mu(x, y)$ [10].

3.2 Feng Thresholding Method

Feng's thresholding method [8] is improved from Wolf et al. [9] thresholding approach in order to tolerate different degrees of illumination unevenness. This method uses two local windows: a primary and a secondary window with the former contained within the latter. The values of local mean $\mu(x, y)$, local standard deviation $\sigma(x, y)$ and minimum gray level M , are calculated in the primary local window and the dynamic range of standard deviation R_σ is calculated in the secondary larger window. The threshold value $T(x, y)$ in a local window is obtained from

$$T(x, y) = (1 - \alpha_1)\mu(x, y) + \alpha_2 \left(\frac{\sigma(x, y)}{R_\sigma} \right) (\mu(x, y) - M) + \alpha_3 M \quad (3)$$

where $\alpha_2 = k_1 (\sigma(x, y)/R_\sigma)^\gamma$, $\alpha_3 = k_2 (\sigma(x, y)/R_\sigma)^\gamma$, and α_1, γ, k_1 and k_2 are positive constants. γ is set to 2 and α_1, k_1 and k_2 are in the ranges of [0.1 0.2], [0.15 0.25] and [0.01 0.05], respectively.

3.3 Algorithms Complexity

Computing $\mu(x, y)$ and $\sigma(x, y)$ in a direct way results in a computational complexity of $O(W^2M \times N)$ for an $M \times N$ image. In order to speed up the computation, an efficient way of computing local means and variances using sum tables (integral images) is proposed in [11, 12] and applied for Sauvola thresholding in [10] so that, the computational complexity does not depend on the window dimension anymore, reducing thus, the computational complexity from $O(W^2M \times N)$ to $O(M \times N)$. Indeed, for our application which deals with online pipeline inspection, it is important to speed-up the image and video analysis algorithms since slow inspection systems lead to extended pumping downtime where, the cost incurred through lost production would be dramatic. So, the use of integral image in this paper permits to the corrosion detection process based on Sauvola and Feng thresholding methods to be faster since less downtime means more working time and then, more benefits.

4 Experiments

4.1 Software Interface Presentation

We have developed software dedicated to the detection of corrosion where an interactive interface, illustrated in Fig. 3, permits to (1) load the video of our interest, (2) choose the size of the adaptive thresholding window W , (3) choose the values of Sauvola and Feng methods parameters given in Eqs. (2) and (3), namely $k, R, \alpha_1, \gamma, k_1, k_2$ and R_σ and (4) finally choose the number of the frames to be processed from the whole video sequence.

Before displaying the segmented frames for both methods, a procedure of processing removal on the area surrounding the disk image, representing the deep

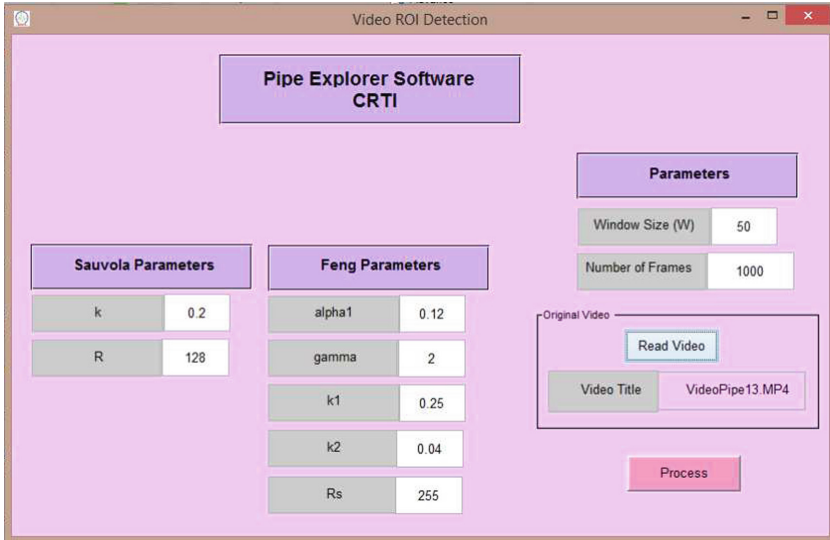


Fig. 3. Presentation of the “Pipe Explorer Software” interface

internal view of the pipeline, is applied (see blue circle in Fig. 4). The processing removal in this area is motivated by the fact that the latter looks very dark since it is very far from the embedded camera and the lighting reaching it is low. Furthermore, the considered regions are gradually processed as the motorized vehicle progresses in the pipeline.

4.2 Region Uniformity Measure

The uniformity of a feature over a region is inversely proportional to the variance of the values of that feature evaluated at every pixel belonging to that region [13]. In this paper, the region uniformity measure U , used to evaluate the segmentation method performance, is given by

$$U = 1 - \frac{w_0\sigma_0^2 + w_1\sigma_1^2}{\sigma_{max}^2} \quad (4)$$

where (w_0, σ_0) and (w_1, σ_1) are (area ratio, variance) of the foreground and the background regions, respectively; whilst σ_{max}^2 is the maximum image variance given by $(f_{max} - f_{min})^2/2$. The highest (near to 1) is the value of U , the highest is the thresholding quality.

4.3 Results and Discussion

For the test, we have chosen a video sequence obtained by the embedded camera, composed of 1000 frames and stored on a section of water transport pipeline

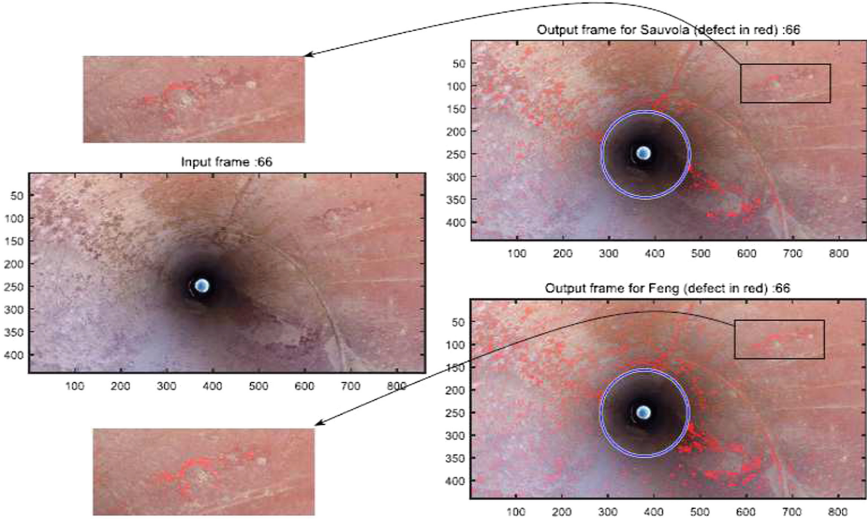


Fig. 4. Sauvola and Feng thresholding results for frame 66

presenting localized attacks of corrosion. The red spots displayed on the output frames representing the risky areas are obtained by Sauvola and Feng thresholding methods. As example, the results for frame 66 are illustrated in Fig. 4. The comparison between the methods of Sauvola and Feng in terms of proportion of damaged areas and thresholding evaluation based region uniformity measure, for all the 1000 images composing the acquired video sequence, are provided by the graphs of Fig. 5a and b, respectively.

It appears from both pictures and graphics that the Sauvola method slightly under-segments the input image compared to the Feng method as shown in Fig. 4 where visually, some parts of the defect indications are missed in the case of Sauvola thresholding. As reported in Table 1, this can be confirmed by the

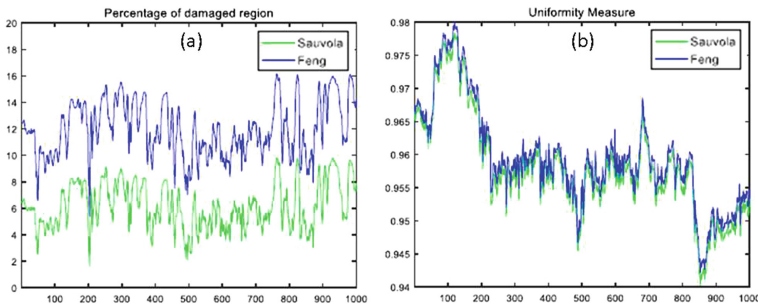


Fig. 5. (a) Percentage of damaged region areas and (b) uniformity measures for methods of Sauvola and Feng on the whole video sequence

Table 1. Sauvola and Feng results for all the 1000 frames

	Sauvola		Feng				
Window size	50		50				
Parameters	k	R	α_1	γ	k_1	k_2	R_s
	0.2	128	0.12	2	0.25	0.04	255
Damaged region							
Range (%)	[1.6% 9.8%]		[5.4% 16.2%]				
Average (%)	6.2%		12%				
Unif. measure							
Range	[0.940 0.978]		[0.942 0.980]				
Average	0.958		0.960%				

measure of the proportions of the damaged region area (colored in red) in regards of the whole processed input image for Sauvola and Feng methods, which are about 5.1% and 10.3%, respectively. The case of frame 66 is valid for all the frames of the video sequence where, the damaged region percentages vary, for Sauvola, in the range of [1.6% 9.8%] with an average of 6.2% whereas, it varies, for Feng, in the range of [5.4% 16.2%] with an average of 12%. Regarding the thresholding performance evaluation, the average values of uniformity measure, on all the video frames, is slightly better for Feng ($U \approx 0.960$) than for Sauvola ($U \approx 0.958$). It is worth to note a possible presence of false positive indications which overestimate the corrosion such as the spiral welding joint in Fig. 4. That said, it is imperative to compare these results with those obtained by an expert for their validation and in order to guide the choice of the thresholding parameters.

5 Conclusion

In this paper, a modern visual equipment “Endoscope” to inspect the interior part of the pipe is used. It consists in a motorized engine embedding a CCD camera. Here, the endoscope is controlled using FPGA technology. A video sequence acquired from a water transport pipeline, presenting mainly corrosion indications, is analyzed and interpreted. Through dedicated software, the indications of corrosion are extracted using two image thresholding methods: Sauvola and Feng. The results are then quantified in terms of area ratio of possible damaged region and in terms of thresholding evaluation measures. To conclude, it reveals from the results that the complex nature of such images requires to the image and video processing techniques to be evaluated in a supervised manner, i.e. by using a ground truth provided by an expert. In other words, a realistic corrosion detection and interpretation should take into account a priori knowledge on the objects composing the internal view of a pipeline such as welding joint, land deposit, stones, stains and soils, which could drastically influence the final interpretation results. These last remarks will be deeply investigated in future works.

Acknowledgments. This research was supported by CRTI as part of technological development of research products with a socio-economic impact. We thank all the team members of project “Pipeline Inspection by Endoscopy” who have participated in the realization of the “Endoscope” which make possible the acquiring of video sequences in pipeline and then their processing; the subject of the study in this paper.

References

1. The free dictionary by Farlex. <http://www.thefreedictionary.com/corrosion>
2. Yasir, M.: Introduction to FPGA Technology (2011). Website FPGA related.com, <https://www.fpgarelated.com/showarticle/17.php>
3. Soler, L., Malandrin, G., Delingette, H.: Segmentation automatique: application aux angioscanners 3D du foie. *Traitement de Signal* **15**(5), 411–431 (1998)
4. Lee, S.U., Chung, S.Y., Park, R.H.: A comparative performance study of several global thresholding techniques for segmentation. *Comput. Vis. Graph. Image Process.* **52**, 17–190 (1990)
5. Sezgin, M., Sankur, B.: Survey over image thresholding techniques and quantitative performance evaluation. *J. Electron. Imaging* **13**(1), 146–165 (2004)
6. Sauvola, J., Pietikainen, M.: Adaptive document image binarization. *Pattern Recogn.* **33**(2), 225–236 (2000)
7. Niblack, W.: *Introduction to Digital Image Processing*. Prentice Hall (1986)
8. Feng, M.L., Tan, Y.P.: Contrast adaptive binarization of low quality document images. *IEICE Electron. Express* **1**(16), 501–506 (2004)
9. Wolf, C., Jolion, J.M.: Extraction and recognition of artificial text in multimedia documents. *Pattern Anal. Appl.* **6**(4), 309–326 (2004)
10. Shafait, F., Keysers, D., Breuel, T.M.: Efficient implementation of local adaptive thresholding techniques using integral images. In: *Document Recognition and Retrieval XV, Proceedings of SPIE, San Jose, CA, vol. 6815* (2008)
11. Crow, F.: Summed-area tables for texture mapping. *ACM SIGGRAPH Comput. Graph.* **18**, 207–212 (1984)
12. Viola, P., Jones, M.: Rapid object detection using a boosted cascade of simple features. In: *Proceedings of IEEE Computer Society Conference on Computer Vision and Pattern Recognition, Kauai, HI, USA, pp. 511–518* (2001)
13. Levine, M.D., Nazif, A.M.: Dynamic Measurement of Computer Generated Image Segmentations. *IEEE Transactions on Pattern Analysis and Machine Intelligence* **7**(2), 155–164 (1985)